Auto-alignment system design for the AEI 10 m prototype facility

Fumiko Kawazoe for the GEO-ISC group

May 2010

This document describes the AEI 10 m Prototype interferometer Auto-Alignment design work which was done from January to April, 2010 as part of the GEO-ISC group.

TABLE OF CONTENTS

Chapter 1

INTRODUCTION

The AEI 10 m prototype facility will provide a suitable experimental environment for interferometric experiments with their sensitivities limited by the fundamental quantum noise. One such experiments, the Sub-SQL interferometer, will be the first to be tested inside the prototype. Its design sensitivity reaches a level of $10^{-19}\,\mathrm{m}/\sqrt{\mathrm{Hz}}$ at 50 Hz dropping to below $10^{-20}\,\mathrm{Hz}/\sqrt{\mathrm{Hz}}$ at 1 kHz, allowing a gap between the Standard Quantum Limit by a factor of 3. Although the limiting noise sources are the suspension thermal noise, radiation pressure noise by the intensity fluctuation of the laser, and the coating thermal noise, reducing all of the known classical noise sources is vital for meeting the required level. The laser frequency noise is will be focused from here on. In order to suppress the laser frequency noise to the required level, which is about a factor of 8 below the design sensitivity, the sub-SQL interferometer will utilize an external cavity called a frequency reference cavity. It is a ring cavity, with each mirror suspended as a triple pendulum. Use of the external cavity instead of its own arm cavities is necessary, since the sub-SQL interferometer will use very light mirrors ($\sim 100\,g$) with relatively large circulating power inside the arm cavities ($600\,W$), so that they are susceptible to radiation pressure noise. The frequency reference cavity will then provide an input laser with the frequency noise suppressed to a level of $10^{-4}\,\mathrm{Hz}/\sqrt{\mathrm{Hz}}$ at 20 Hz dropping to below $10^{-6}\,\mathrm{Hz}/\sqrt{\mathrm{Hz}}$ at 1 kHz. In order to achieve this level the laser frequency is locked to the frequency determined by the reference cavity's optical length. However angular fluctuations of the mirrors also need to be controlled to optimize operating conditions. Therefore, the alignment control design has to be developed. The proposed design of the alignment control system for the reference cavity is described in this document. From here on the system is called the auto-alignment control. It should be noted that this is one plan that we like to test for the first phase of the experiment. The plan is flexible, so that we are not strictly limited to only use the current

plan, rather we have more choices. However thanks to the GEO-ISC collaboration. the current plan encompasses rich experiences gained by the people working with the GEO 600 detector, which gives grounds for the decision to use the current plan in the first run of the experiment.

Chapter 2

THE AUTO-ALIGNMENT CONTROL

2.1 The concept

The purpose of the auto-alignment control is to obtain the increased accuracy of optimum operating conditions for the reference cavity. The plan is to use a similar method that the GEO 600 detector uses [2], [1]. The signals necessary for the auto-alignment system will only be available when the longitudinal degree of freedom (DOF) is controlled , therefore from here on we assume that the longitudinal DOF is already controlled. The optimum operating conditions are met when the alignment of the incoming beam and that of the eigenmode of the reference cavity match (this requires controlling 4 DOFs; angular in two directions, and lateral in two directions), and the absolute alignment of the cavity eigenmode is kept ideal (this requires controlling 6 DOFs; 2 angular per mirror, or one could also think of the absolute 4 DOFs, and 2 DOFs (rotational around the axis of the incoming beam, and shift in x-y plane), as shown in Fig. 2.1. We aim to obtain such conditions by controlling the axis of the incoming beam to match the cavity eigenmode, and by controlling the beam spot positions on the cavity mirrors, respectively. The two control systems will be described in the following sections.

In addition, the GEO 600 detector uses an auxiliary system (so called the beam centering control) to control the directions of the two outgoing beams that are detected to obtain DWS signals, so that they always hit the center of quadrant photo-detectors (QPDs). It ensures correct DWS signals . The control bandwidth of this system is high ($\sim 1\,\mathrm{kHz}$), ensuring correct DWS signals whenever the longitudinal DOF is controlled. However we will not use such a system for our first phase, yet we will leave space for installing the beam centering system in case we might need it. This decision is made based on the fact that the reference cavity will be placed on a optical table which is supported by a Seismic Attenuation System (SAS), and the rms motion of the optics at the pendulum frequency ($\sim 1\,\mathrm{Hz}$)is expected

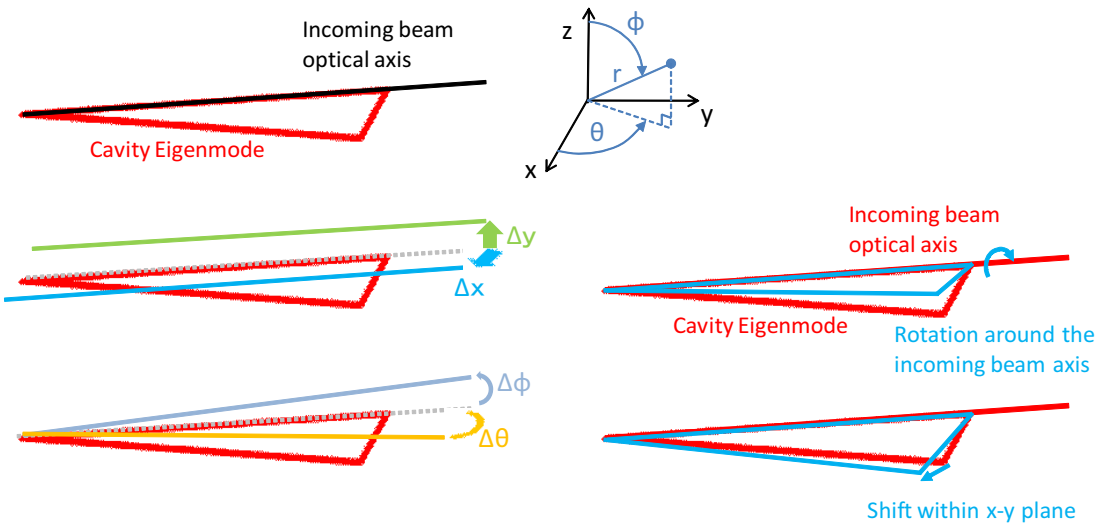

Figure 2.1: Angular degrees of freedom that are controlled by the auto-alignment system. There are 10 DOFs. Four of them are the relative alignment between the cavity eigenmode and the axis of the incoming beam, that are shown in the left half. Once the cavity eogenmode and the incoming beam axis match, what is left are the same 4 DOFs, but in the sense of absolute alignment, and remaining two DOFs are the rotational DOF around the axis of the incoming beam, and the lateral shift within the x-y plane, as shown in the right column of the figure.

to be much smaller than the GEO 600. Therefore we expect that the rms deviations on the spot positions on the QPDs are small enough that they do not contaminate the DWS signals.

2.2 Relative alignment

The Differential Wavefront Sensing (DWS) scheme [2], [1] will be used for controlling the axis of the incoming beam so that it matches the cavity eigenmode. The plan is to prepare two steering mirrors that are suspended as a single pendulum, that guide the beam which is tapped off from the sub-SQL interferometer path into the reference cavity, and to actuate on them. Use of steering mirrors is chosen for the DWS control because it will allow faster control than the case where the cavity mirrors (suspended as a triple pendulum) are used, since they have two more suspension stages. We aim the control bandwidth of about 5 Hz with this method. In order to verify if correct feed-back signals can be obtained, and if the two steering mirrors can be actuated correctly, two calculations were performed with a simulation tool developed by G. Heinzel.[4]. The first simulation calculates how misaligning each cavity mirror will cause the cavity eigenmode to change compared to the aligned case. It shows what DWS error signals the two QPDs will be able to provide. (The reason why two QPDs are used will be described in the following subsection.) The second simulation then calculates how the steering mirrors will be actuated to null the DWS error signals. Each will be described in the following subsections.

2.2.1 Cavity misalignment types

Table 2.1, and 2.2 show how a misalignment of each cavity mirror will change the cavity eigenmode. Here each cavity mirror (Ma, Mb, and Mc) are slightly misaligned (by $10\,nrad$) in yaw and pitch directions. A case where Ma is misaligned in the yaw direction is shown in Figure 2.2 as an example. Throughout this document, the misalignment angles are expressed as $\alpha_{a,b,c}$ for the yaw direction, and $\beta_{a,b,c}$ for the pitch direction, with each subscript representing the corresponding mirror. For each mirror's misalignment, a cavity eigenmode change is recorded as spot position changes on the mirrors, $(\Delta x, y, z)$, a change in the waist location $(\Delta x, z)$, the angle of the outgoing beam from the cavity leak, and the promptly

reflected beam, each with respect to the aligned case (γ for the yaw direction, and δ for the pitch direction), the relative angle between the cavity leak and the promptly reflected beam, and finally the characteristic of the misalignment at the waist. The characteristic of the cavity misalignment indicates a ratio between a lateral shift and a angular shift of the waist position. In order to obtain a DWS signal, a difference between the Pound-Drever Hall signal from each half of the QPDs is computed. Due to this process, when the signal is obtained in the vicinity of the waist, a demodulated signal is maximized when the misalignment at the waist is the pure angular type, or $\Theta^W = 90°$. In order to be sensitive to the pure lateral shift type of misalignment, one can modify this amount by adding 90° to it, by e.g. propagating the outgoing beam further, or inserting lenses. (Lenses that are used to adjust Gouy phase is called Gouy phase lenses from here on, and they will be described in the following section.) Then two split photo-detectors are placed, with a relative Gouy phase difference set to be 90° between the two by inserting a set of Gouy lenses in front of one of the two QPDs. Then they give two different information about the misalignment; one mainly contains the information regarding lateral shifts at the waist, the other mainly angular shifts.

The misalignment of Ma and Mc create very similar effects, therefore instead of treating them separately, we treat them as a combined mirror and consider a common and a differential misalignment. The two sets of two tables show that the two DOFs, namely α_+, and β_-, will make very small signals(i.e. they will cause zero lateral shift of the waist position, and almost zero angle between the cavity leaked beam and the promptly reflected beam.) Therefore they will not be controlled by the DWS scheme. But it will be shown that they appear as spot position shifts on the QPDs, and from there the remaining two DOFs can be controlled, which will be described in the section of spot positioning control.

2.3 Gouy phase lenses

As briefly mentioned in the following section, in order to obtain full information on the cavity misalignment one needs two QPDs, each being sensitive to the angular misalignment type and the lateral shift misalignment type, in terms of what happens at the waist. We uses Gouy phase lenses for that purpose. With the lenses the beam at the the QPD will

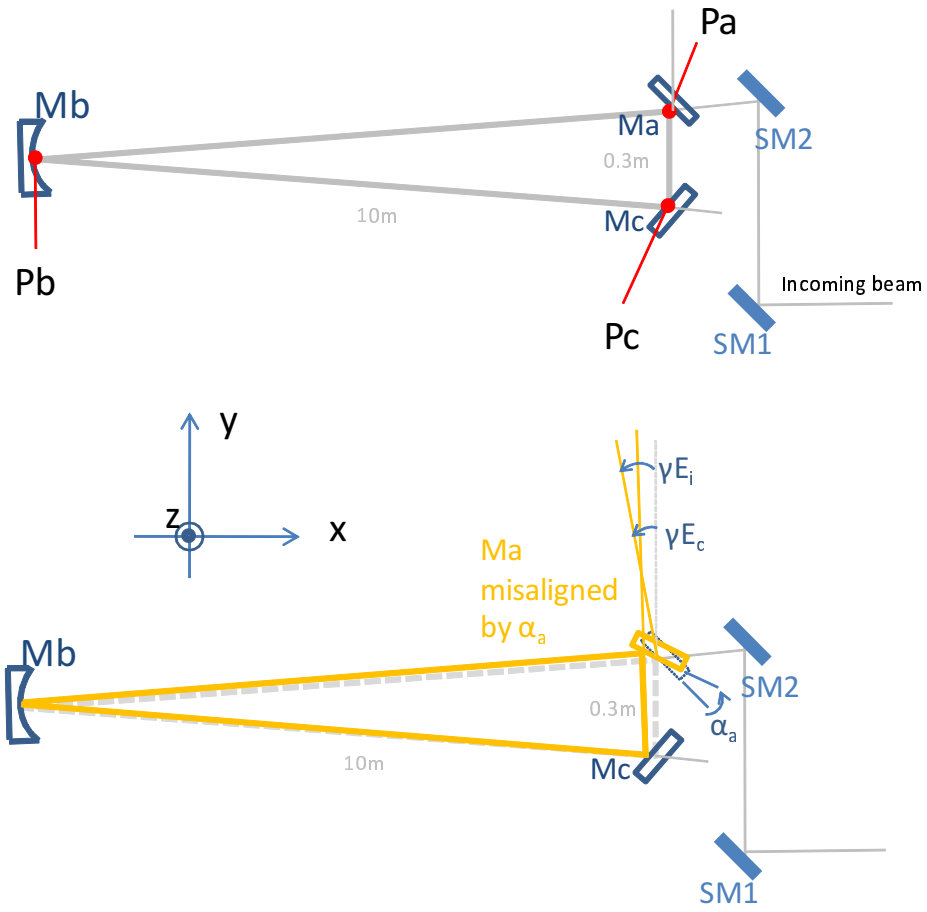

Figure 2.2: Cavity eigenmode of the aligned case and an example of a misaligned case. Here Ma is misaligned by the angle α_a.

acquire an additional Gouy pahse shift between the Hermite-Gaussian fundamental mode and the second higher-order mode by 90°. Figure 2.3 shows what kind of lenses can be used, and where they are located, and the beam radius change, and the Gouy phase shift as the beam propagates through the lenses from the first waist to the QOD. The first lens is a converging lens with a focal length of $60\,cm$, it will create a very small waist. Then placing a diverging lens (focal length of $-3\,cm$)a little bit before the new focus, and placing the QPD at some chosen distance from the second lens, one can achieve a relative Gouy phase shift of 90° between the QPDs and where the first lens is positioned. Thus one can place

Cause	P_a Δx	P_a Δy	P_b Δy	P_c Δx	P_c Δy
α_a	$-10.202\,m \cdot \alpha_a$	$10.051\,m \cdot \alpha_a$	$0.205\,m \cdot \alpha_a$	$-9.900\,m \cdot \alpha_a$	$-9.754\,m \cdot \alpha_a$
α_b	$0.205\,m \cdot \alpha_b$	$-0.202\,m \cdot \alpha_b$	$-13.974\,m \cdot \alpha_b$	$-0.205\,m \cdot \alpha_b$	$-0.202\,m \cdot \alpha_b$
α_c	$9.900\,m \cdot \alpha_c$	$-9.754\,m \cdot \alpha_c$	$0.205\,m \cdot \alpha_c$	$10.202\,m \cdot \alpha_c$	$10.051\,m \cdot \alpha_c$
α_-	$-10.051\,m \cdot \alpha_-$	$9.903\,m \cdot \alpha_-$	$0.000\,m \cdot \alpha_-$	$-10.051\,m \cdot \alpha_-$	$-9.903\,m \cdot \alpha_-$
α_+	$-0.151\,m \cdot \alpha_+$	$0.149\,m \cdot \alpha_+$	$0.205\,m \cdot \alpha_+$	$0.151\,m \cdot \alpha_+$	$-0.149\,m \cdot \alpha_+$

Cause	Waist Δx	E_c γE_c	E_i γE_i	Relative angle $\gamma E_c - \gamma E_i$	Θ^W
α_a	$-10.051\,m \cdot \alpha_a$	$1.005 \cdot \alpha_a$	$2 \cdot \alpha_a$	$1.005 \cdot \alpha_a$	$59.2°$
α_b	$0.000\,m \cdot \alpha_b$	$-1.370 \cdot \alpha_b$	$0 \cdot \alpha_b$	$-1.370 \cdot \alpha_b$	$-90°$
α_c	$10.051\,m \cdot \alpha_c$	$1.005 \cdot \alpha_c$	$0 \cdot \alpha_c$	$-0.995 \cdot \alpha_c$	$59.5°$
α_-	$-10.051\,m \cdot \alpha_-$	$0.000 \cdot \alpha_-$	$1 \cdot \alpha_-$	$-1.000 \cdot \alpha_-$	$59.4°$
α_+	$0.000\,m \cdot \alpha_+$	$1.005 \cdot \alpha_+$	$1 \cdot \alpha_+$	$0.005 \cdot \alpha_+$	$90°$

Table 2.1: Diffrential Wavefront Sensing signals-in yaw direction

the other OPD equivalent to where the first lens is to have two QPDs that carry sufficient information of the cavity misalignment. At the same time one needs to take care so that the beam spot on the QPD is something of a usable size. Here we set the radius to be $2\,mm$. As shown in Fig. 2.3, the first Gouy lens (GL1) will focus the beam to a very small waist, and the Gouy phase change around the newly formed focus is very steep in the vicinity

Cause	P_a Δz	P_b Δz	P_c Δz
β_a	$-19.665\,m \cdot \beta_a$	$-26.930\,m \cdot \beta_a$	$-19.876\,m \cdot \beta_a$
β_b	$37.800\,m \cdot \beta_b$	$37.800\,m \cdot \beta_b$	$37.800\,m \cdot \beta_b$
β_c	$-19.876\,m \cdot \beta_c$	$-26.930\,m \cdot \beta_c$	$-19.665\,m \cdot \beta_c$
β_+	$-19.770\,m \cdot \beta_-$	$-26.930\,m \cdot \beta_-$	$-19.770\,m \cdot \beta_-$
β_-	$0.106\,m \cdot \beta_+$	$0.000\,m \cdot \beta_+$	$-0.106\,m \cdot \beta_+$

Cause	Waist Δz	E_c δE_c	E_i δE_i	Relative angle $\delta E_c - \delta E_i$	Θ^W
β_a	$-19.770\,m \cdot \beta_a$	$0.702 \cdot \beta_a$	$1.43 \cdot \beta_a$	$-0.728 \cdot \beta_a$	$32.02°$
β_b	$37.800\,m \cdot \beta_b$	$0.000 \cdot \beta_b$	$0.000 \cdot \beta_b$	$0 \cdot \beta_b$	$0°$
β_c	$-19.770\,m \cdot \beta_c$	$-0.702 \cdot \beta_c$	$0.000 \cdot \beta_c$	$-0.702 \cdot \beta_c$	$31.08°$
β_+	$-19.770\,m \cdot \beta_+$	$0.000 \cdot \beta_+$	$0.714 \cdot \beta_+$	$-0.714 \cdot \beta_+$	$31.52°$
β_-	$0.000\,m \cdot \beta_-$	$0.702 \cdot \beta_-$	$0.714 \cdot \beta_-$	$-0.012 \cdot \beta_-$	$-90°$

Table 2.2: Diffrential Wavefront Sensing signals-in pitch direction

of the waist. For example, placing GL1 3mm before the ideal point will change the total Gouy phase by 13 degrees. (Placing it 3mm closer to GL2 would only cause 0.5 degrees oof change because in this case, the Gouy phase between GL1 and GL2 increases while it will be decreased between the PD and GL2 and they cancel out each other). Therefore one has to adjust the lens position to within a few mm. The distance from the first waist (the cavity

waist) and the first lens is $\sim 1.7\,m$. The design comes from the concern that we might need to control the beam so that it always hits the center of the QPDs, and for that this leaves enough space for placing a set of optics needed for the beam centering system.

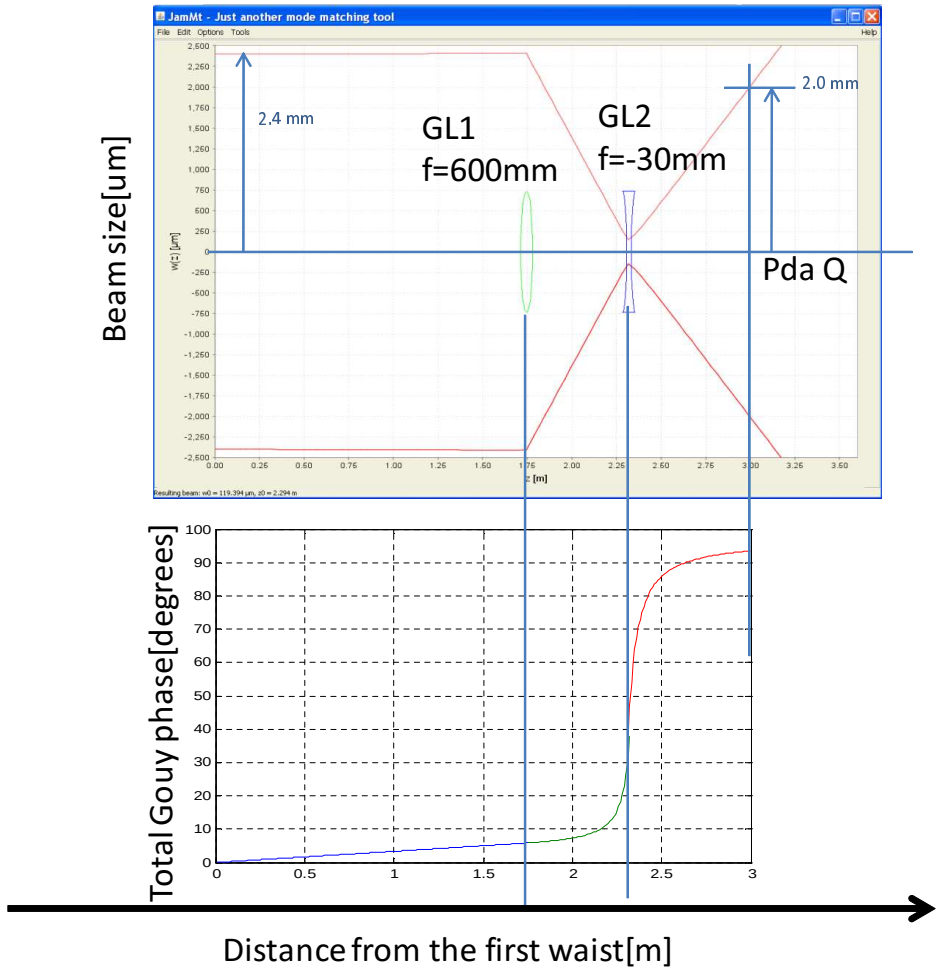

Figure 2.3: Differential Wavefront Sensing signals on two photodetectors whose Gouy phase are orthogonal to each other.

2.4 Steering mirror actions

Since our plan is to prepare two steering mirrors that are suspended as a single pendulum, and to use it as actuators for the DWS DOFs, one needs to calculate how they should be

actuated. Figure 2.4 shows the concept of how the DWS signals are detected and being used to control the relative alignment via actuating on two steering mirrors.

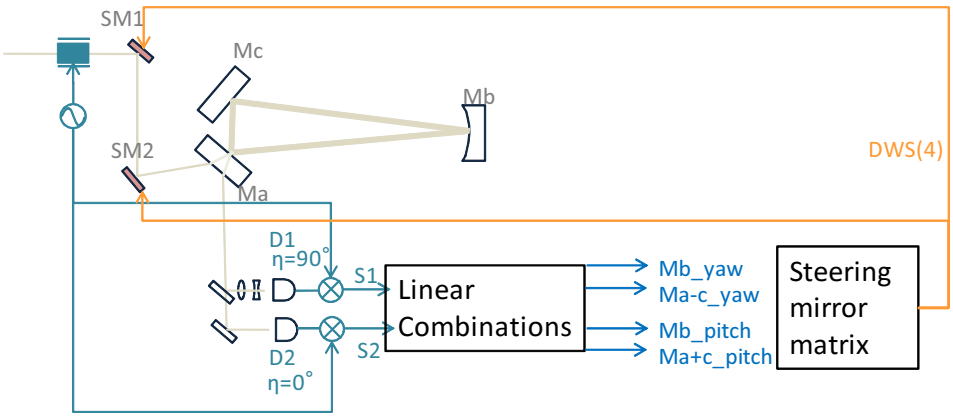

Figure 2.4: Differential Wavefront Sensing signals on two photodetectors whose Gouy phase are orthogonal to each other.

Two QPDs are placed at the detection port. One (D2)is sensitive to the angular misalignment type, while the other (D1)is made to be sensitive to the lateral misalignment type by adjusting the Gouy phase with the use of two lenses. If we set the Gouy phase of 90° by the lenses the signals from the two photo-detectors will be given by

$$S_{D1} = -0.592 \cdot \alpha_- \tag{2.1}$$

$$S_{D2} = -1.370 \cdot \alpha_b - 1.000 \cdot \alpha_- + 0.005 \cdot \alpha_+ \tag{2.2}$$

for signals in yaw direction, and

$$S_{D1} = 2.226 \cdot \beta_b - 1.164 \cdot \beta_+ \tag{2.3}$$

$$S_{D2} = -0.714 \cdot \beta\_0.012 \cdot \beta_- \tag{2.4}$$

for signals in pitch direction. In both directions, taking proper linear combinations will allow one to obtain four signals that are only sensitive to $\alpha_b, \alpha_-, \beta_b$, and β_+, since α_+, and β_- are both very small and negligible, this will not be controlled by this method. These four signals will be multiplied by factors that are necessary for steering mirrors to be actuated

properly. The factors can be found in the table below. 2.3. This was also simulated by the c code.[4]

Cause	SM1 yaw	SM2 yaw	SM1 pitch	SM2 pitch
α_b	$0.146 \cdot \alpha_b$	$0.831 \cdot \alpha_b$	$0.000 \cdot \alpha_b$	$0.000 \cdot \alpha_b$
α_-	$9.070 \cdot \alpha_-$	$9.570 \cdot \alpha_-$	$0.000 \cdot \alpha_-$	$0.000 \cdot \alpha_-$
β_b	$0.000 \cdot \beta_b$	$0.000 \cdot \beta_b$	$46.904 \cdot \beta_b$	$-46.558 \cdot \beta_b$
β_+	$0.000 \cdot \beta_+$	$0.000 \cdot \beta_+$	$24.267 \cdot \beta_+$	$-23.588 \cdot \beta_+$

Table 2.3: Steering mirror matrix

2.5 Spot position control

So far we have seen that the four DOFs can be controlled by the DWS scheme. In order to control the remaining six DOFs, three QPDs will be used to detect spot positions. We plan to use the cavity mirror as actuators for this system, and aim the control bandwidth of about 0.1 Hz. In principle, placing each right behind each mirror, and readout the spot positions on each of them should give sufficient information. However we plan to position them as shown in Fig. 2.5. One (PD2) is placed at the back of the second steering mirror (SM2), another (PDb) at the back Mb, and the other being one of the QPDs whose AC part of the signals are already in use for the DWS scheme. Although the one that is behind SM2 is not directly sensing the spot position on a cavity mirror, it is equivalent of doing so because the input beam is controlled to match the cavity eigenmode with the DWS control. There are two QPDs that are used for the DWS control, we plan to choose the one that has the Gouy lenses inserted in the path, since it is likely to be more sensitive due to the magnification set by them (however it is not always so, because a general misalignment is a mixture of a lateral shift and an angular change, and depending upon how they are combined, one can get a reduced signal size due to the lenses). Tables 2.4, and 2.5 show how cavity mirrors misalignment will cause spot positions to change. Pda I, and Pda Q are the ones that are used for the DWS signals, with Pda Q having lenses inserted in the

beam path. For a comparison purpose PDc is also placed behind Mc, but the information it carries do not need to be used. The results depend on the distances between the input mirror and SM2, and between SM1 and SM2, but due to the limited space on the optical table, the distances cannot be changed dramatically. Thus even though those distances are subject to change, the results are not expected to change much.

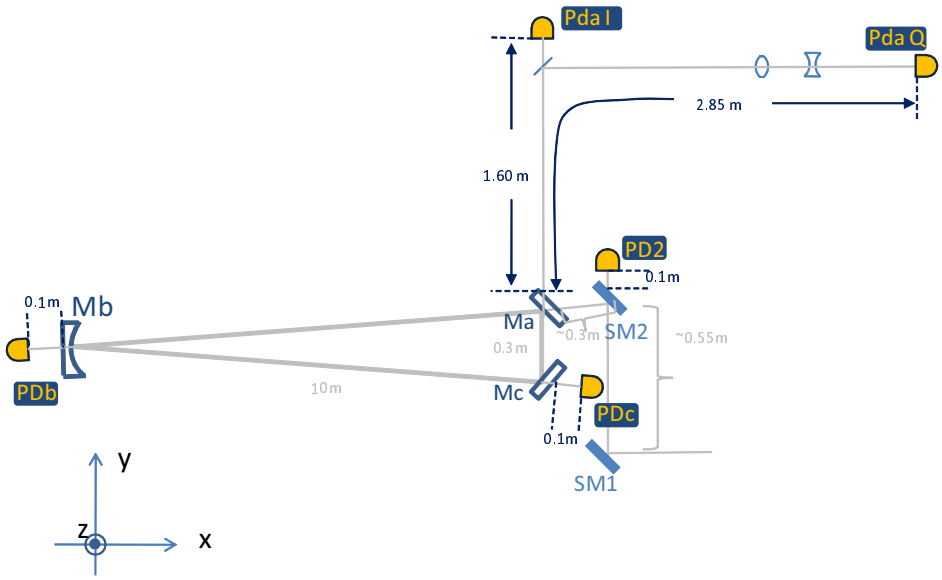

Figure 2.5: Detecting spot positioning signals on three QPDs.

Cause	PD2	PDa I	PDa Q	PDb	(PDc)
α_a	$13.106\,m \cdot \alpha_a$	$11.861\,m \cdot \alpha_a$	$10.206\,m \cdot \alpha_a$	$-0.072\,m \cdot \alpha_a$	$-10.027\,m \cdot \alpha_a$
α_b	$0.227\,m \cdot \alpha_b$	$-2.426\,m \cdot \alpha_b$	$-18.977\,m \cdot \alpha_b$	$14.194\,m \cdot \alpha_b$	$-0.033\,m \cdot \alpha_b$
α_c	$-12.697\,m \cdot \alpha_c$	$-8.270\,m \cdot \alpha_c$	$17.645\,m \cdot \alpha_c$	$-0.341\,m \cdot \alpha_c$	$10.356\,m \cdot \alpha_c$
α_+	$0.205\,m \cdot \alpha_+$	$1.796\,m \cdot \alpha_+$	$13.926\,m \cdot \alpha_+$	$-0.207\,m \cdot \alpha_+$	$0.165\,m \cdot \alpha_+$
α_-	$12.902\,m \cdot \alpha_-$	$10.065\,m \cdot \alpha_-$	$-3.720\,m \cdot \alpha_-$	$0.135\,m \cdot \alpha_-$	$-10.192\,m \cdot \alpha_-$

Table 2.4: Spot positioning signal for yaw direction

Similar to the DWS signal case, adding and subtracting signals form various QPDs will

Cause	PD2	PDa I	PDa Q	PDb	(PDc)
β_a	$24.706\,m \cdot \beta_a$	$18.496\,m \cdot \beta_a$	$-17.020\,m \cdot \beta_a$	$27.071\,m \cdot \beta_a$	$19.778\,m \cdot \beta_a$
β_b	$48.068\,m \cdot \beta_b$	$37.800\,m \cdot \beta_b$	$-13.969\,m \cdot \beta_b$	$37.845\,m \cdot \beta_b$	$37.800\,m \cdot \beta_b$
β_c	$25.010\,m \cdot \beta_c$	$21.023\,m \cdot \beta_c$	$2.415\,m \cdot \beta_c$	$27.068\,m \cdot \beta_c$	$19.542\,m \cdot \beta_c$
β_+	$24.858\,m \cdot \beta_+$	$19.760\,m \cdot \beta_+$	$-7.303\,m \cdot \beta_+$	$27.070\,m \cdot \beta_+$	$19.660\,m \cdot \beta_+$
β_-	$-0.152\,m \cdot \beta_-$	$-1.264\,m \cdot \beta_-$	$-9.718\,m \cdot \beta_-$	$0.002\,m \cdot \beta_-$	$0.118\,m \cdot \beta_-$

Table 2.5: Spot positioning signal for pitch direction

allow one to form linearly independent signals that are clean in terms of signal mixture. One set of example of such combinations are shown in the following equations.

$$SP_{\alpha_b} = 1.000 \cdot \mathrm{PDb} \tag{2.5}$$

$$SP_{\alpha_+} = 0.206 \cdot \mathrm{PD2} + 0.750 \cdot \mathrm{PDaQ} + 1.000 \cdot \mathrm{PDb} \tag{2.6}$$

$$SP_{\alpha_-} = 1.000 \cdot \mathrm{PD2} \tag{2.7}$$

$$SP_{\beta_b} = 2.830 \cdot \mathrm{PD2} - 0.045 \cdot \mathrm{PDaQ} - 2.611 \cdot \mathrm{PDb} \tag{2.8}$$

$$SP_{\beta_+} = -0.291 \cdot \mathrm{PD2} + 0.05 \cdot \mathrm{PDaQ} + 0.371 \cdot \mathrm{PDb} \tag{2.9}$$

$$SP_{\beta_-} = 0.291 \cdot \mathrm{PD2} + 1.000 \cdot \mathrm{PDaQ} \tag{2.10}$$

Each combination will contain one DOF, that can be applied to the cavity mirrors accordingly to realize the spot position control.

2.6 Summary

Figure 2.6 shows the schematic overview of the auto-alignment system. Numbers indicate the DOFs. The EOM is used to create a control sideband, and it is the same one used for the longitudinal DOF. The modulation frequency will be about 30 Hz.

Figure 2.7 shows where the auto-alignment system fits in the Prototype facility. The reference cavity input mirrors will be placed inside the middle tank, and the end mirror inside the South tank. The detection bench and the middle tank is separated by about 1.2 m, leabing about 50 cm to reserve the space for the possible installation of the beam centering devices (Galvos, two polarizing beam splitters, and a half wave plate in each path).

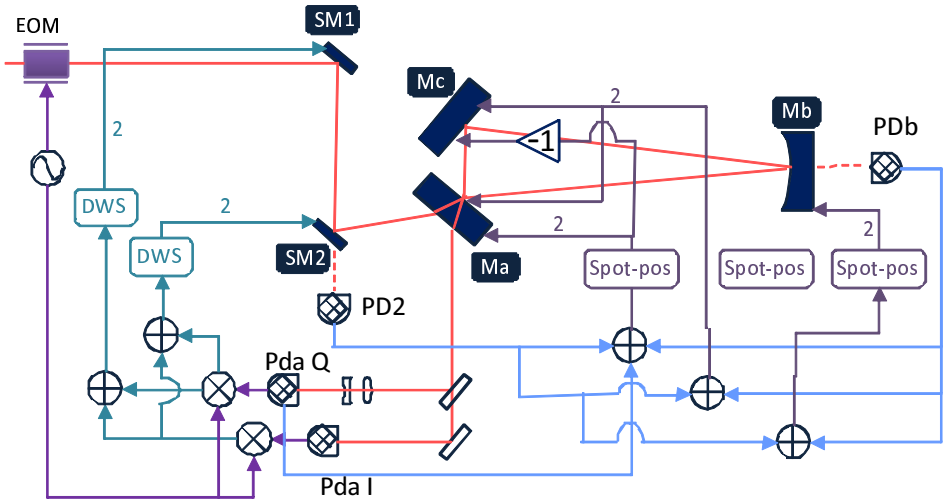

Figure 2.6: Schematic overview of the auto-alignment control system. Numbers indicate the DOFs.

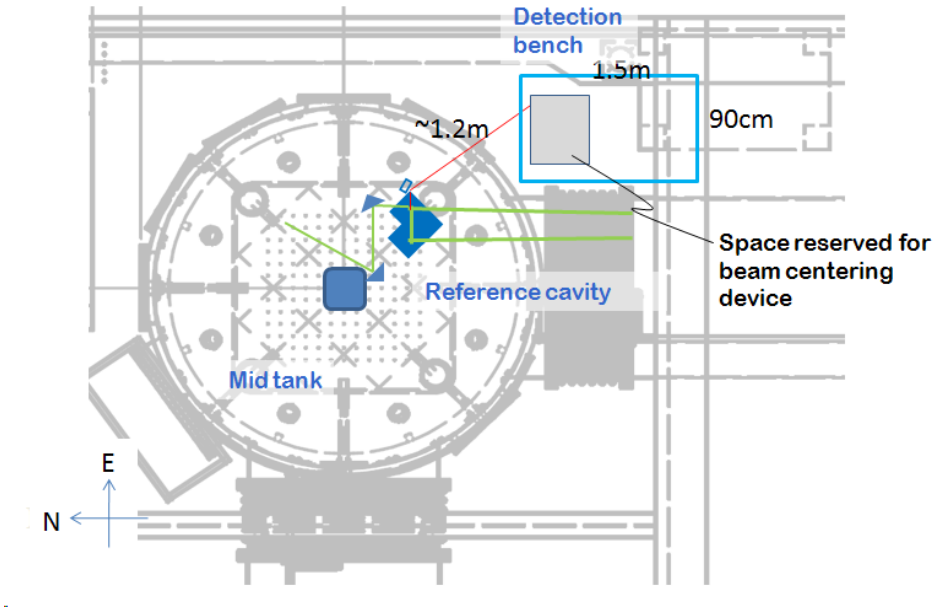

Figure 2.7: Auto-alignment system location. Mainly it is centered around the middle tank.

Appendix A

DWS SIGNAL DOUBLE CHECK WITH FINESSE

DWS signals are double checked with FINESSE [3] and it matches the result from the c-code, as shown in TableA.1.

Cause	PDa I	PDa Q	Θ^W
α_a	$-1.07 \cdot 10^{-5}$	$-6.69 \cdot 10^{-6}$	58.0
α_b	$-1.49 \cdot 10^{-5}$	$1.61 \cdot 10^{-7}$	-89.4
α_c	$1.09 \cdot 10^{-5}$	$6.53 \cdot 10^{-6}$	59.1
β_a	$7.80 \cdot 10^{-6}$	$-1.23 \cdot 10^{-5}$	-32.4
β_b	0	$2.39 \cdot 10^{-5}$	0
β_c	$-7.35 \cdot 10^{-6}$	$-1.25 \cdot 10^{-5}$	-30.5

Table A.1: DWS signals with FINESSE, the result match the result from the c-code.

Appendix B

GEOMETRICAL ANALYSES

It is worth while to check results on tables 2.1, and 2.2 with geometrical analyses. Here misalignment type of α_b, α_-, β_b, β_+, are geometrically analyzed. The other two, α_+, and β_- are not. This is because the former four can be analyzed by projecting them onto a linear cavity, and it is simpler, while the latter two cannot be explained by such a method, making it more difficult to imagine a 3D eigenmode.

B.1 α_b *misalignment*

This is a misalignment of Mb in yaw. A major feature of this type of misalignment is that the waist position stays unchanged regardless of the misalignment. This can be understood by the following reasonings.

In Fig. B.1 there are two pictures. The top shows the aligned case (red), and the misaligned case (light red). Due to the misalignment, a beam spot on Mb is shifted. First we assume that the waist position stays unchanged, i.e. the beam is tilted at the waist. When one tries to draw a triangle that passes through the waist, applying Snell's law in each reflection, one finds a correct triangle, which is the new eigenmode. However, in addition if there was also a lateral shift to the waist position, as shown in the bottom figure with green lines, one will not find a correct triangle anymore. This is because adding the additional lateral shift does not changes of incidence on the two flat mirrors, as expressed with two parallel marks in the figure, as a result the sharpest point of the triangle will not be created on the curved mirror anymore. Therefore it can be concluded that with α_b type of misalignment the waist position stays the same as the aligned case. Then the beam angle at the waist, as well as the spot position change on Mb can be calculated when we follow the following steps. In Fig. B.2, we name the angle between the bottom lines of the two triangle θ. Then due to Snell's law, the angle at the waist is θ. We name half the smallest angle

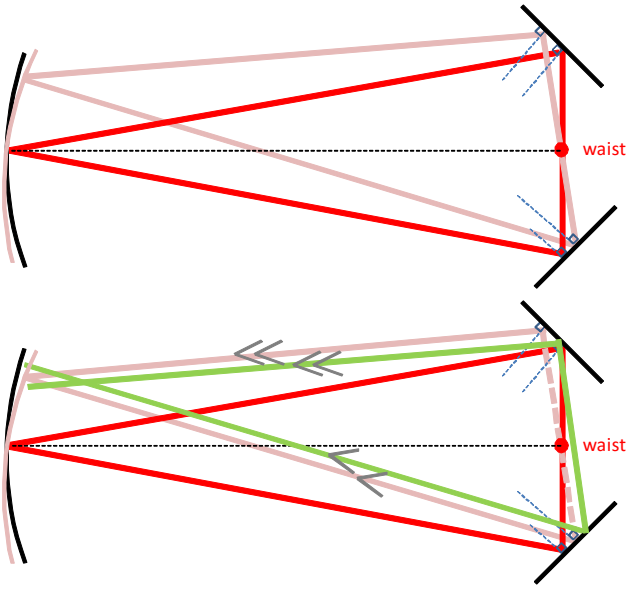

Figure B.1: (Top)Waist stays unchanged with α_b type of misalignment. (Bpttom)Had there been a shift in the waist position, one cannot draw a triangle correctly as shown by a green lines.

of the original triangle ϕ. Then due to the misalignment, one of the two broader angles will bet larger, while the other smaller by the same amount $2\alpha_b$, leaving ϕ constant. Then comparing the yellow shaded triangle and the gray one, one can see that the other smaller angle of the gray shaded triangle is also θ. If we know the point where a diameter that connects the beam spot on Mb and the misaligned radius of curvature (ROC)(the green cross), crosses the original, we can calculate dY, and θ. The bottom drawing shows that such a point is distance d away from the waist position along the original normal vector of Mb. Which can be understood with a following reasoning. We name half the shortest side of the original triangle d (indicated by the black arrow). Since θ is very small compared to one, the shortest side of the misaligned triangle is still $2d$. The diameter that connects the misaligned radius of curvature and the beam spot on Mb intersects the shortest side where it divides the side into half, (indicated by the pink arrow) because the angle ϕ is very small. However the distance between the waist and the beam spot position (indicated by the orange arrow) changes by $\theta \cdot d$(indicated by the light blue arrow). Then the distance

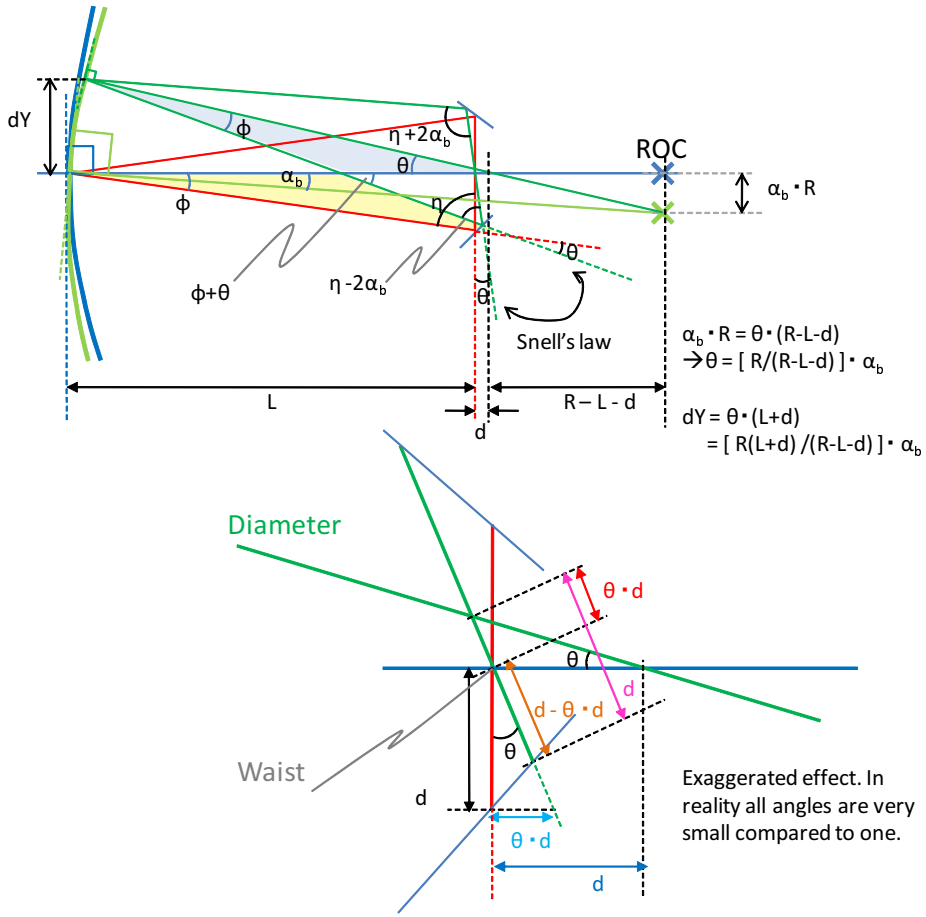

Figure B.2: Beam angle at the waist, as well as the spot position change on Mb can be calculated with applying Snell's low

between the waist position and the crossing point along the shortest side of the misaligned triangle (indicated by the red arrow) is $\theta \cdot d$ because it is a length difference between the pink and the orange arrows. Then since we know that the angle between the diameter and the original normal vector(the blue line) is θ from the previous reasonings, we know that the distance along the normal vector between the waist and where the diameter crosses the normal vector is d. (indicated by the blue arrow). Finally dY, and θ can be given by

$$\theta = \frac{\alpha_b \cdot R}{R - L - d} \tag{B.1}$$

$$dY = \frac{\alpha_b \cdot R}{R - L - d}(L + d) \tag{B.2}$$

Substituting the numerical values that were used in the simulation codes($R = 37.8, L = 10.05, d = 0.15$) they give following values. $\theta = 1.370 \cdot \alpha_b$, and $dY = 13.970 \cdot \alpha_b$. They match the simulation results.

B.2 α_- *misalignment*

This is a misalignment of differential Ma and Mc in yaw. A major feature of this type of misalignment is that the it only gives a lateral shift at the waist waist and not an angular change because the geometrical change it creates is symmetric between the two longer sides of the triangle. The amount by which the beam shifts at the waist can be calculated by taking the following steps. In Fig. B.3, in the aligned case (shown by the blue triangle) we name the two big angles θ. By the differential misalignment of the two mirrors, each by the amount $\alpha_-/2$, the eigenmode will change into one that is shown by the red triangle. Smells law tells that the two big angles change by α_-, resulting in the change in the small angle by $2 \cdot \alpha_-$. Thus the angle deviation between the long side (given as $d\phi$) equals to half the α_-. Therefore the waist shift (given as dX) is given by

$$dX = \alpha_- \cdot L \tag{B.3}$$

Substituting the numerical value, it gives $dX = 10.05 \cdot \alpha_-$, which matches the simulation result.

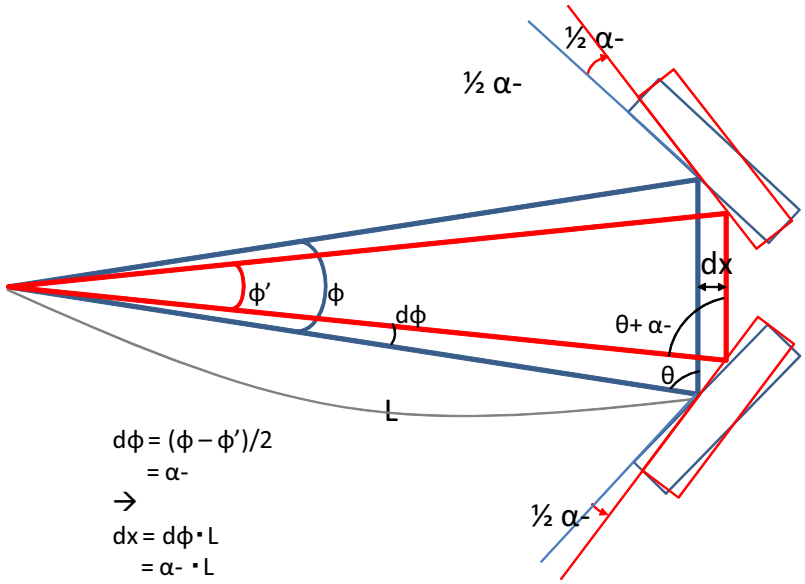

Figure B.3: Due to geometrical symmetry that α_b type of misalignment creates, change in eigenmode is symmetric on both of the longer sides of the triangle. This results in creating the change in lateral shift at the waist and no angular change.

B.3 β_b *misalignment*

This is a misalignment of Mb in pitch. A major feature of this type of misalignment is that the it shifts the whole eigenmode in horizontal direction (When pitch is defined as a tilt in horizontal direction). In Fig. B.4, the triangle cavity is projected onto a linear cavity. This is possible because of the very small angle of incidence on Mb ($\sim 0.5°$). The two flat mirrors Ma, and Mc overlap one another in this picture. The original eigenmode is given by the blue horizontal line. When Mb is misaligned by β_b, the ROC will move by the distance $\beta_b \cdot R$. One can draw a line from the new ROC, intersecting Mc or Ma perpendicularly (indicated by the green horizontal line), then the line also intersects the misaligned Mb (indicated by the red curve) perpendicularly, due to the definition of ROC. Then this is the new eigenmode. The amount to which it shifts from the original eigenmode (dZ) is given by

$$dZ = \beta_b \cdot R \tag{B.4}$$

Substituting the numerical value, it gives $dz = 37.8 \cdot \beta_b$, which matches the simulation result.

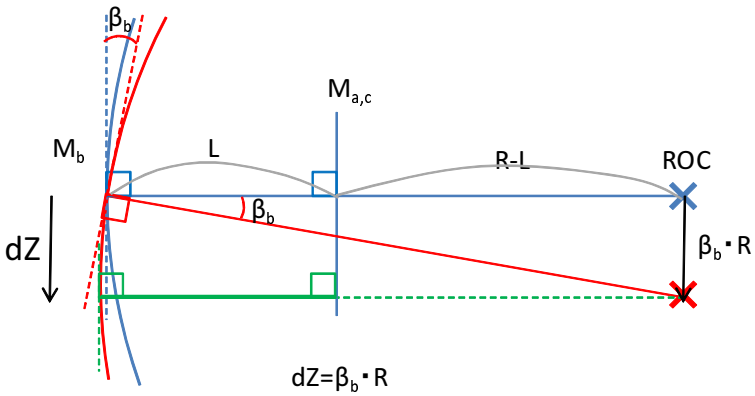

Figure B.4: Due to the fact that the angle of incidence at Mb is very small, $beta_b$ type of misalignment can be projected onto a linear cavity. When Mb tilts in pitch by β_b ROC will be shifted, causing the eigenmode to shift the same amount.

B.4 β_+ *misalignment*

This is a common misalignment of Ma and Mc in pitch. A major feature of this type of misalignment is that the it gives both the angular and the lateral shift at the waist. In Fig. B.5, the triangle cavity is projected onto a linear cavity. However, due to the fact that the angle of incidence on Mc and Ma is big ($\sim 45°$), misaligning each by $\beta_+/2$ in pitch appears the same as misaligning the input mirror by a smaller amount $\beta_{eff}/2$ in the linear cavity. When the input mirror is misaligned by $\beta_{eff}/2$, one can draw a line from the ROC, intersecting the input mirror perpendicularly (given by the red line), then it intersects the end mirror perpendicularly (by the definition of ROC). Then it is the new eigenmode. Therefore one can calculate where it hits the end mirror (dXe), and the input mirror(dXi), as they are given by

$$dXi = \frac{\beta_{eff}}{2} \cdot (R - L) \tag{B.5}$$

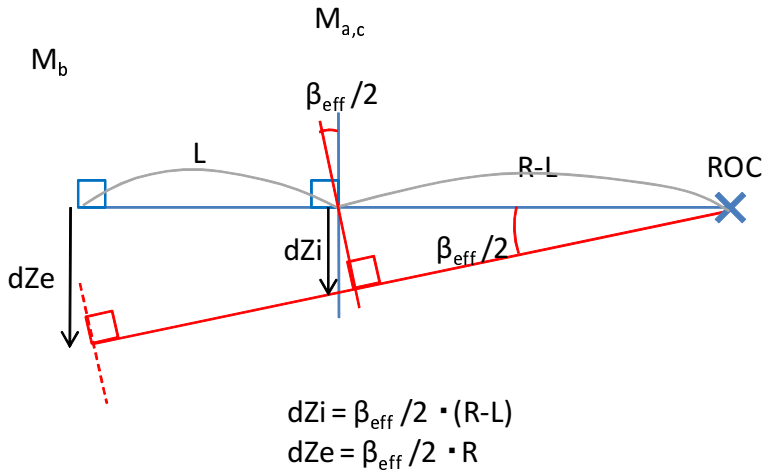

Figure B.5: This type of misalignment can be projected onto a linear cavity. However, due to the fact that the angle of incidence on Mc and Ma is big ($\sim 45°$), misaligning each by $\beta_+/2$ in pitch appears the same as misaligning the input mirror by a smaller amount $\beta_{eff}/2$ in the linear cavity.

$$dXe = \frac{\beta_{eff}}{2} \cdot R \tag{B.6}$$

β_{eff} is given by $\beta_{eff} = \frac{\beta_+}{\sqrt{2}}$. This can be understood by following the reasonings shown in Fig. B.6. The incident beam on Ma or Mc can be decomposed into two directions ; one that is parallel to the mirror surface and the other that is perpendicular to it, as shown by the top left picture. When the mirror is tittled by $\beta_+/2$, according to Snell's law the parallel component will not be deflected by the misalignment, and the perpendicular component will be deflected by β_+ with respect to the aligned mirror's normal vector, as shown by the top right picture. Due to the fact that the incident beam is only partly deflected, the total deflection angle should be smaller than β_+. To calculate the total deflection angle, it is useful to use a spherical coordinate, as shown by the bottom left picture. The total beam (indicated by the red arrow) points down by the amount β_{eff}, which can be calculated geometrically as shown in the bottom right picture, and is given by

$$\beta_{eff} = \frac{1}{\sqrt{2}}\beta_+ \tag{B.7}$$

Substituting numerical values to equations B.5, andB.6, one obtains $dXi = 19.622 \cdot \beta_+$, and $dXe = 26.729 \cdot \beta_+$, which match the simulation results.

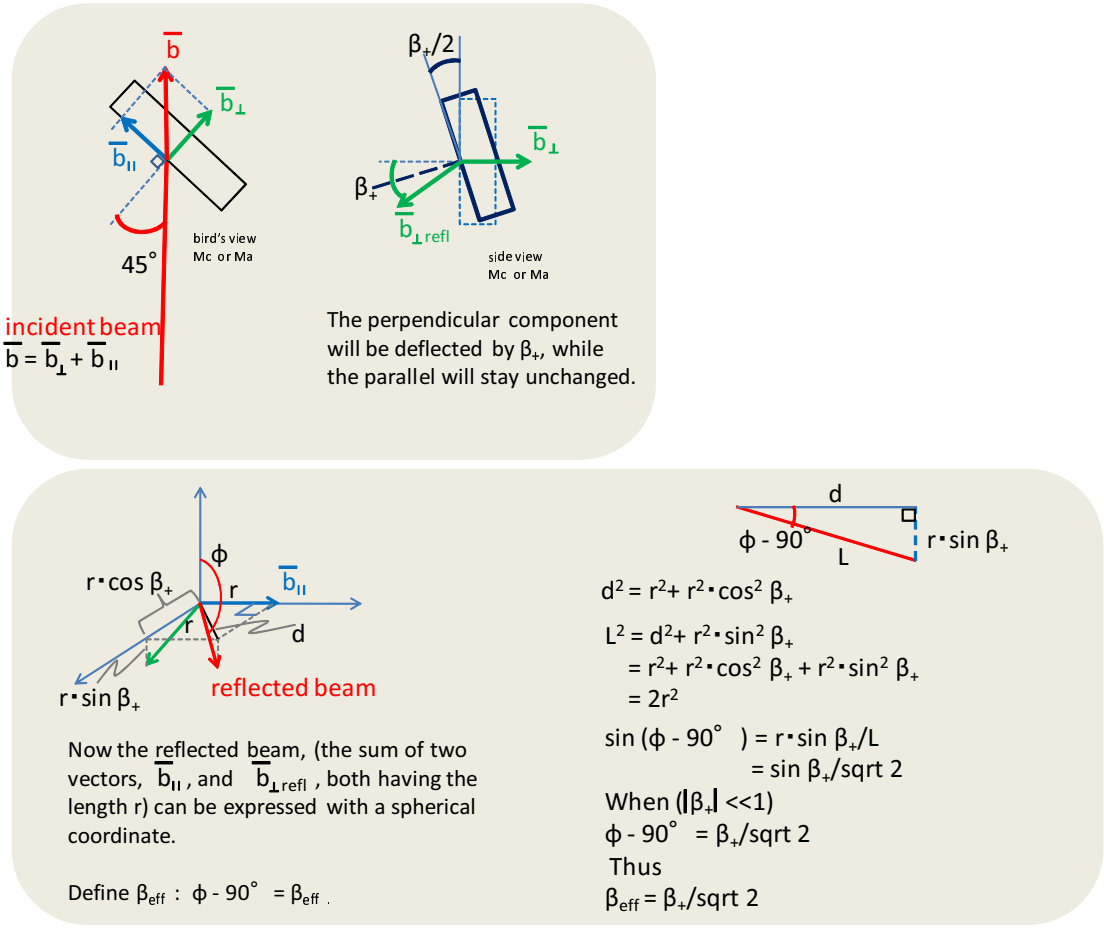

Figure B.6: Due to the large angle of incidence, when Ma and Mc is misaligned in pitch by $\beta_+/2$ the beam reflected on Ma or Mc will be partly deflected. This gives difference between the actual misalignment angle and the effective misalignment angle which is $\beta_{eff}/2$.

Appendix C

SIMULATION CODES

C codes can be found at

`http://geo-isc.physics.gla.ac.uk/doku.php?id=more_on_aa_for_the_reference_cavity`

because they are too long to put them here.

```
# Laser
l laser 1 0 n1


# Define the modulation sidebands
s s1 0 n1 n2
mod eom1 30M 0.3 3 pm n2 n3 # GEO MC
s s2 0 n3 n5

# ring cavity

bs bs1 0.9995 0.00045 0 44.284 n5 n7 n6 n8
bs bs2 0.99994  0.00001 0 1.433  n9 n10 n11
n12 #curved
bs bs3 0.9997  0.00025 0 44.284 n13 n14 n15
n16

s sL1 10.434 n6 n9
s sL2 10.434 n10 n13
s sL3 0.3 n8 n14

attr bs2 Rc 37.8

cav c1 bs2 n9 bs2 n10    # Define cavity
eigenmode

maxtem 3

###############

#fsig sigmby bs2 ybeta 0.0001 0 10n  #pitch Mb
#fsig sigmc bs3 ybeta 0.0001 0 10n # pitch Mc
#fsig sigma bs1 ybeta 0.0001 0 10n # pitch Ma
### Does not work
attr bs3 ybeta 10n


#fsig sigmby bs2 xbeta 0.0001 0 10n  #pitch Mb
#fsig sigmc bs3 xbeta 0.0001 0 10n # pitch Mc
#fsig sigma bs1 xbeta 0.0001 0 10n # pitch Ma
### Does not work
#attr bs3 xbeta 10n

########demodulation phase check
######run3:xaxis QPD1 phase lin -180 180 180
# at 0 it is max, OK.
######run3:put QPD2 phase $x1
######run3:diff bs2 xbeta


# Set up beamsplitter for detection stage

s s3 0 n7 n18

bs bs5 0.5 0.5 0 45 n18 n19 n20 dump
s s4 0 n19 n21
s s5 0 n20 n22

attr s3 g 0
attr s4 g 0
attr s5 g 90

trace 8

# power detectors
#pd pcav n10 # ok, it is resonant
#pd pref n7

## how about demodulation phase?
#run3:xaxis pref phase lin -180 180 180
#run3:diff bs2 phi
#pd1 pref 30M 0 n21 # should be 0 it seems.


xaxis s3 gx lin 0 90 100
put* s3 gy $x1

### Set up quadrant photodiodes
#pd2 QPD1 30M 0 0.0001 0 n21  # QPD with
Gouy phase 0
#pdtype QPD1 y-split
#pdtype QPD1 x-split

pd1 QPD1 30M 0 n21
pdtype QPD1 y-split
#pdtype QPD1 x-split


yaxis lin abs
#gnuterm no
gnuterm windows
multi
pause
```

Figure C.1: DWS by FINESSE

BIBLIOGRAPHY

[1] H Grote. *Making it Work: Second Generation Interferometry in GEO600 !* PhD thesis, University of Hannover, 2003.

[2] G Heinzel. *Advanced optical techniques for laser-interferometric gravitational-wave detectors*. PhD thesis, University of Hannover, 1999.

[3] http://www.gwoptics.org/finesse/. an interferometer simulation tool.

[4] ifocad by G. Heinzel. beam tracing tool.